Homogeneity of Oxide Air-Sphere Crystals from Millimeter to 100-nm Length Scales: A Probe for Macroporous Photonic Crystal Formation

Lydia Bechger* and Willem L. Vos†

Department of Science and Technology, and MESA+ Research Institute, University of Twente, P.O. Box 217, NL-7500 AE Enschede, The Netherlands

Received December 23, 2003. Revised Manuscript Received April 2, 2004

We study the homogeneity of photonic air-sphere crystals made of oxides. This important class of macroporous materials is prepared via liquid precursor infiltration of opal templates and subsequent removal of the template by calcination. We have synthesized highly ordered structures of macropores in a solid backbone consisting of two consecutively infiltrated materials: the oxide pairs zirconia/titania (ZrO_2/TiO_2) and alumina/titania (Al_2O_3/TiO_2). The ordered arrangement of the air spheres was confirmed by scanning electron microscopy. To determine the spatial distribution of the materials, energy-dispersive spectroscopy was used. It was observed that there are variations in the distribution of oxide materials throughout the sample on length scales ranging from 1 mm to 100 nm. We propose that the spatial variations originate from the reaction process where the precursors hydrolyze and possibly also from the densification that occurs in the calcination step. Since many light emitters are quenched on semiconductor surfaces, such inhomogeneities hamper a proper shielding of the emitters, thereby impeding spontaneous emission experiments in photonic crystals. On the other hand, inhomogeneities appear to cause minor variations in the optical Bragg conditions.

Introduction

The development of porous materials is a subject of intensive research. Well-known structures such as zeolites are widely used in every day life including desiccants, pet litter, and powdered laundry detergents.[1] Recently, macroporous materials, that is, materials with pore radii larger than 25 nm, are under intense scrutiny for their great potential to novel applications in separation science, catalysis,[2] and in particular photonic materials.[3−5]

Photonic crystals are three-dimensional composites of dielectric materials with a periodicity on length scales of the wavelength of light. Because of the periodic variation of the refractive index, the photonic crystal shows optical Bragg diffractions, which can lead to a photonic band gap: a frequency range for which light will not propagate in any direction. Currently, these crystals receive a lot of attention for their possibility to completely control spontaneous emission of dye and other internal light sources, and the propagation of light.[6,7] An advantageous way to make photonic crystals is to use artificial opals as a template and invert their structure to obtain so-called inverse opals or air-sphere crystals. These inverted structures consist of interconnected air spheres in a solid backbone that exhibits a high refractive index.

Electron microscopy is probably the most widely used technique to characterize the backbone of (oxide) air-sphere crystals. It is a reliable technique since it visualizes the macroporous structure, clearly illustrating the discrete air spheres. This technique, however, determines only the surface characteristics. Optical techniques, for example, reflectivity and transmission experiments, probe larger areas of the crystal.[8] Wijnhoven et al. were the first to explore air-sphere crystals with X-ray experiments.[9] With X-ray absorption volume fractions were determined and small-angle X-ray scattering was used to examine long-range order in three dimensions. Although all these techniques are very important for studying the backbone of air-sphere crystals, they cannot be used for homogeneity characteristics. Inhomogeneities especially need attention when the backbone of air-sphere crystals consists of two different materials. The spatial distribution of these two materials is then of high importance. Conversely, the study of possible inhomogeneities will also yield new

* To whom correspondence should be addressed. E-mail: l.bechger@tnw.utwente.nl. URL: www.photonicbandgaps.com

† E-mail: w.l.vos@utwente.nl. URL: www.photonicbandgaps.com.

(1) Davis, M. E. *Nature* **2002**, *417*, 813−821.

(2) Proceedings of the 2nd International Symposium on Mesoporous Molecular Sieves (ISMMS). Bonneviot, L., Giasson, S., Kaliaguine, S., Stöcker, M., Eds. *Microporous Mesoporous Mater.* **2001**, *44*−*45*.

(3) Norris, D. J.; Vlasov, Y. A. *Adv. Mater.* **2001**, *13*, 371−376.

(4) Stein, A. *Microporous Mesoporous Mater.* **2001**, *44*−*45*, 227−239.

(5) Koenderink, A. F.; Johnson, P. M.; Galisteo-Lopez, J. F.; Vos, W. L. *C. R. Phys.* **2002**, *3*, 67−77.

(6) Yablonovitch, E. *Phys. Rev. Lett.* **1987**, *58*, 2059−2062.

(7) John, S. *Phys. Rev. Lett.* **1987**, *58*, 2486−2489.

(8) Vos, W. L.; van Driel, H. M.; Megens, M.; Koenderink, A. F.; Imhof, A. In *Photonic Crystals and Light Localization in the 21st Century*; Soukoulis, C. M., Ed.; Kluwer Academic Press: Dordrecht, The Netherlands, 2001; pp 191−218.

(9) Wijnhoven, J. E. G. J.; Bechger, L.; Vos, W. L. *Chem. Mater.* **2001**, *13*, 4486−4499.

10.1021/cm035373o CCC: $27.50
Published on Web 05/15/2004

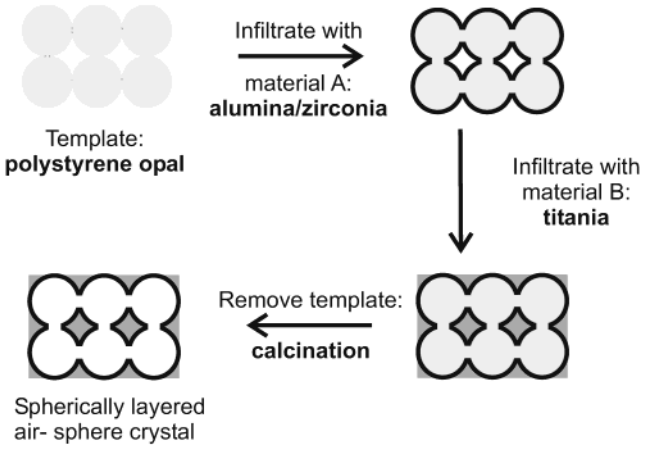

Figure 1. Schematic drawing of the principle of the preparation of spherically layered mixed oxide air-sphere crystals. The artificial opal is first infiltrated with a precursor of one oxide, e.g., alumina, silica, or zirconia, before it is infiltrated with another oxide, e.g., titania. After calcination an air-sphere crystal is expected to consist of two materials with a spherically layered shell structure.

information on the formation of large macroporous assemblies consisting of pure materials.

On mesoporous (1 nm < r < 25 nm) and microporous (r < 1 nm) scales, Raman et al. have already explored the formation of metal oxides on template surfaces at a molecular level.[10] They have investigated the formation of mesoporous silicas where the pore morphology is dependent on preparation circumstances such as concentration of the reactants, aging conditions, and molecular interactions between template and reactant. To the best of our knowledge, however, nobody has ever taken such a close look at the process of macroporous (r > 25 nm) structure formation. We are the first to explore the process of air-sphere crystal formation, by studying inhomogeneities.

Previously, we have already observed inhomogeneities with the naked eye during liquid precursor infiltration; that is, some parts of the crystal change color from white to grayish during the infiltration while other parts remain white.[9] Usually, these white parts were visible in the upper part of the crystal, and if precursor was added from the top, the remaining white parts could be infiltrated after all. These differences in infiltration already indicate that the infiltration is not always uniform on the millimeter scale, the typical length scales of opals.

To investigate the homogeneity of inverse opals, we have prepared samples consisting of two oxides. The principle of this sample preparation is illustrated in Figure 1. The starting material is the same as that for the pure titania (TiO_2) air-sphere crystal, an artificial opal consisting of monodisperse polystyrene spheres. The first step is the infiltration of the opal with the precursor of one oxide, in this particular example alumina (Al_2O_3) or zirconia (ZrO_2). Jiang et al.[11] have demonstrated that infiltration and reaction of alkoxides on similar polystyrene substrates is surface templating.[12] In our experiments we have also detected that infiltration and reaction of alkoxides resulted in a layer oxide covering the polystyrene spheres.[9,13] All these observations confirm that alkoxides generally have a good wetting on polystyrene spheres. The second step is the infiltration of the remaining air voids with another oxide, in this case titania, which deposits on the already present insulating oxide layer. The third and final step is the removal of the template by calcination during which the polystyrene is burned away and an air-sphere crystal with a spherically layered structure is expected. Studying the composition of this expected structure will provide information about the inhomogeneity.

Electron-dispersive spectroscopy (EDS) is a good technique for investigating inhomogeneities in air-sphere crystals made of mixed oxides. A high-energy electron beam hits a certain sample area and the present elements radiate characteristic X-rays. By application of this technique in combination with scanning electron microscopy (SEM), areas can be probed with several hundreds of micrometers in cross section. EDS in combination with transmission electron microscopy (TEM) can even probe on a single air-sphere level, that is, about 100 nm.

Although the technique of spherically layered mixed oxide air-sphere crystals appears to be very suitable to investigate the homogeneity of inverse opals, it was originally developed to create efficient emission from light sources in photonic air-sphere crystals.

If an infiltration is first done with an insulating material followed by an infiltration with a high index semiconductor such as titania, a spherically layered air-sphere crystal is expected of an insulating oxide layer on the inner surface of a high refractive index contrast backbone (see Figure 1). This thin insulating layer prevents the electron transfer from the excited state of the internal light source (e.g., dye) to the conduction band of the semiconductor (e.g., titania). In previous experiments, it has been shown that coating titania powder with a silica layer indeed prevents electron transfer.[14] Above a certain layer thickness the electron transfer is precluded, resulting in efficient emission of laser dye compared to a low quantum efficiency on bare titania. This goal requires a homogeneous infiltration of the precursors.

Experimental Section

The first step of the preparation of mixed oxide air-sphere crystals is the infiltration of the artificial opal, see for detailed template growth and lateral sizes of the template opals refs 9 and 13. To infiltrate the opals, that is, fill the interstitial space between the spheres with a solid material, we have used liquid precursors consisting of an alkoxide diluted with an alcohol: ethanol or propanol. The precursors titanium(IV) propoxide (98%) (TPT), zirconium(IV) propoxide (70% solution in 1-propanol) (TPZ), and aluminum tri-*sec*-butoxide (97%) (TBAl) were purchased from Aldrich. Ethanol (99.5%) was obtained from Merck and 2-propanol (99.5%, anhydrous) from Aldrich. The

(10) Raman, N. K.; Anderson, M. T.; Brinker, C. J. *Chem. Mater.* **1996**, *8*, 1682−1701.
(11) Jiang, P.; Bertone, J. F.; Colvin, V. L. *Science* **2001**, *291*, 453−457.
(12) Zakhidov, A. A.; Baughman, R. H.; Iqbal, Z.; Cui, C. X.; Khayrullin, I.; Dantas, S. O.; Marti, I.; Ralchenko, V. G. *Science* **1998**, *282*, 897−901.
(13) Bechger, L. Ph.D. Thesis, University of Twente, Enschede, The Netherlands, 2003; ISBN 90-365-1991-9.
(14) Bechger, L.; Koenderink, A. F.; Vos, W. L. *Langmuir* **2002**, *18*, 2444−2447.

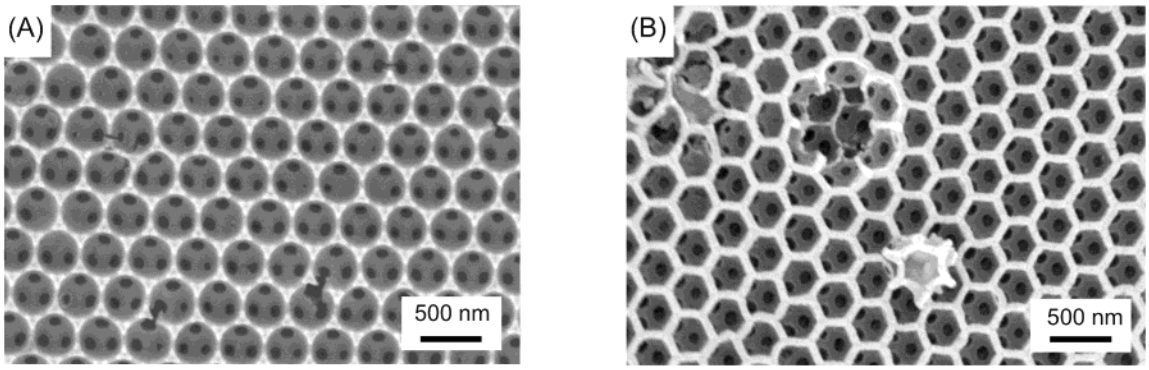

Figure 2. SEM images of two inverse opals consisting of two different materials, respectively, alumina/titania (a) and zirconia/titania (b). The air spheres are well-ordered in the fcc (111) plane. In both images the connecting windows are clearly visible as dark spots. In (a) the interstitial holes can also be seen between each triplet of air spheres, which indicates that surface templating has taken place. The air spheres of (b) look more hexagonal than usual.[9,15] One air sphere has popped out, probably due to heating or handling.

infiltrations were done in a glovebox under nitrogen at room temperature and took typically about 0.5−1 h. After each infiltration the opal is placed in a nitrogen flow for several hours before it is placed in a water-rich environment in ambient conditions to react with water. The infiltrations were performed once (for zirconia) or twice (for alumina) with the respective precursor of the insulator, followed by five or four infiltrations with the precursor of titania (TPT).

To remove the polystyrene template and to crystallize the oxides, the samples were heated to 450 °C in the following way: 0.33 °C/min to 80 °C, 1 h at 80 °C, 1 °C/min to 450 °C, 6 h at 450 °C, and cooling with 10 °C/min.

The SEM images were taken with an ISI DS-130 scanning electron microscope, after sputtering the samples with a thin layer of gold. The spatial measurements (sphere size determination) done on the micrographs were corrected for tilt. Transmission electron microscope images were taken with a Philips CM30 Twin STEM.

EDS−SEM was done with a JEOL JXA-8621 Superprobe at Leiden University, without sputtering the samples with gold. The superprobe was equipped with a single-crystal detector. The characteristic Kα and Lα lines were detected with either a pentaerythritol (PET) or a thalliumacidphthalate (TAP) single crystal. All SEM-EDS measurements were done with a 20-kV electron beam. A typical scan of the emission lines of one element took about 10 min.

EDS-TEM was done with a Philips CM30 TEM, fitted with a Kevex Delta-Plus EDX and based at the Central Materials Analysis Lab at the MESA$^+$ Research Institute. Measurements were done with a 300-kV electron beam. A typical measurement took about 200 s. The X-ray lines were detected through a boron nitride (BN) window on a silicon lithium (SiLi) detector.

Results

The infiltration of the liquid precursors into the opal can be followed by the eye. Air-sphere crystals reveal optical Rayleigh scattering because of the presence of small crystallites. Because of multiple scattering of light from these small grains, the air-sphere crystals appear white. When infiltrating the opal with liquid precursor, the refractive index contrast changes, from solid material/air to solid material/liquid, and as a result a different color, gray, is apparent.

Already in the synthesis of pure oxide air-sphere crystals, it was noticed that the bottom part was usually infiltrated best during the infiltration (see ref 9). Although this problem was overcome by adding precursor from the top, areas were still present where no color change was observed. This illustrates that even on a millimeter scale differences in infiltrations are observed, and therefore inhomogeneous distributions of materials are obvious if applying more than one oxide in several infiltration steps.

In the synthesis of mixed oxide air-sphere crystals, where two materials were applied separately, the same inhomogeneities were observed. Some areas in the opal turned grayish whereas other parts remained white opalescent.

(1) Scanning Electron Microscopy. Figure 2 shows SEM pictures of air-sphere crystals made from two different mixed oxides. Both pictures show well-ordered air spheres in a hexagonal face-centered cubic (fcc) structure. Figure 2a is a top view of the (111) surface plane of an alumina/titania sample made from an $r =$ 238 nm polystyrene template. The radius of the air spheres is 196 ± 2 nm, a shrinkage of ∼18% compared to the template, which is somewhat lower compared to values observed in pure titania air-sphere crystals (26.5 ± 5%).[9] The largest single domain observed in this sample is about 16 × 24 μm, which corresponds to an area of 40 × 60 spheres, comparable to the pure titania air-sphere crystals that were previously made from similar substrates.[15] Connecting windows, clearly seen as black spots in the figure, indicate that the air spheres are connected with the layers beneath. Interstitial holes between the air spheres are also clearly visible, confirming that the infiltration and reaction are surface templating and not volume templating.[15] Figure 2b is a (111) plane of a zirconia/titania air-sphere crystal also made from a polystyrene template with sphere radii of 238 nm. After calcination, a shrinkage of 22% is obtained, resulting in an air-sphere radius of 185 ± 2 nm. The largest domain observed in this sample is about 30 × 30 μm, which corresponds to an area of 80 × 80 spheres. This domain size is similar to sizes found in pure oxide air-sphere crystals. In this SEM picture the windows are also clearly visible. There is a peculiar defect on the surface; one air sphere has popped out of the plane and fits with its shape exactly in the remaining hole. This defect is probably due to heating or handling. The air spheres in this micrograph look more rectangular than round compared to SEM pictures of

(15) Wijnhoven, J. E. G. J.; Vos, W. L. *Science* **1998**, *281*, 802−804.

other air-sphere crystals. This morphology was observed previously by several other groups. Holland et al.[16] also noticed this rodlike structure with pure zirconia inverse opals but did not have a clarification for it. Yan et al.[17] detected a similar skeleton in an iron metal air-sphere crystal prepared by reduction of an iron-oxide (F_2O_3) crystal. They assigned the rod-shaped morphology to enhanced sintering since the process takes place under hydrogen instead of nitrogen. Recently, Dong et al.[18] described such rodlike skeletons in titania. They observed that after one infiltration cycle, the inverse opal shows a rodlike skeleton of the sample. At the surface of the sample, however, a normal shell structure was found. They ascribed the deviating behavior in the particular sample regions to different drying and reaction conditions. The area in SEM image 2b is most probably an external surface and therefore we do not think that this deviation is caused by similar phenomena. Furthermore, since with small-angle X-ray scattering no evidence was observed for such structural deviations,[9] we believe the rodlike skeleton is rather an incidental (surface) feature rather than a usual phenomenon. In a crushed sample prepared for TEM measurements indeed spherical air spheres were visible. From the micrographs it can be seen that successive infiltrations with different oxide precursors results in air-sphere crystals of high quality, comparable to the quality of the pure titania air-sphere crystals.[15]

(2) Energy-Dispersive Spectroscopy with SEM. With EDS it is possible to detect the density of atoms in a sample by the use of characteristic X-rays generated with an electron beam. The intensity of the X-rays is a gauge for the amount of atoms present at a certain area. In this way the distributions of both oxides can be mapped in the air-sphere crystals. In the experiment, we have detected the Kα radiation of aluminum and titanium, at energies of 1.4870 keV (corresponding to a wavelength of 8.34013 Å) and 4.5090 keV (corresponding to a wavelength of 2.74973 Å), respectively. The Lα radiation of zirconium was detected at 2.0420 keV (corresponding to a wavelength of 6.07050 Å). Calibrating the atomic densities of the elements from the emitted intensity is difficult because of the sensitivity of the detector and absorption processes: different elements have different emission wavelengths, and therefore they are absorbed differently by the elements present in the sample. For example, the Kα radiation of aluminum is not absorbed in the same proportion by titanium as the Lα radiation of zirconium. Measurements on the pure elements zirconium, aluminum, and titanium indicated that the detector was less sensitive for the zirconium radiation by roughly a factor of 10. Consequently, we use the measured intensities only as a qualitative gauge.

The excitation volume depends on the porosity and chemical composition of the sample and on the voltage used. The penetration depth can be calculated with a Monte Carlo simulation.[19,20] A porosity of 90% was assumed, based on earlier results,[14] and the chemical composition of the backbone was estimated from the infiltration ratio, which was 23% v/v alumina for the alumina/titania sample and 24% v/v zirconia for the zirconia/titania sample. The excitation volume had roughly the shape of a liquid drop, with a depth between 8 and 10 μm and a width between 6.5 and 7.5 μm, where the widths decrease exponentially with depth. The probe volume is much larger than a single air sphere since we are probing about 20 layers in depth. On the other hand, the probe volume is small enough to distinguish different areas in the samples that have typical lateral sizes between 500 μm and 1 mm.

The upper panels of Figure 3a,b are SEM pictures of respectively alumina/titania and zirconia/titania samples. These pictures show the whole samples and the numbers on each piece show the positions where the EDS measurements were done. Initially, each area was examined with SEM to judge the nature of the area, that is, open or closed air spheres, the presence of bulk material, and order or disorder. Next, the EDS measurements were done at that same position. Figure 3a,b are bar diagrams of the intensities measured at five different positions on each sample and two additional points obtained on other samples. Figure 3a displays data measured on alumina/titania samples. Positions 2, 3, and 4 show a distribution with both materials present. Although the intensities vary a little throughout the sample, the general trend appears to be rather an even distribution of materials. With SEM we determined that these positions revealed open air-sphere structures as in Figure 2a. Positions 1 and 5 consist of areas where the structure did not contain open air-sphere structures but areas covered with bulk material. As can be seen from the bar diagram, the intensity of titanium at these positions is very high compared to the intensity of aluminum, so we conclude that the bulk material at these positions mainly consists of titania. Positions 6 and 7 are measured on a different sample, made in the same preparation batch. Position 7 was an open air-sphere structure with a lot of disorder. There is some signal of aluminum in addition to the main component titanium. Position 6 was an area covered mainly with bulk material. The main component of this area is titanium.

In Figure 3b the measured intensities on zirconia/titania samples are shown. Since the sensitivity of the detector for zirconium was much less, we have multiplied all the intensities of zirconium with a factor of 10. Positions 1, 2, 4, and 5 were determined with SEM to be open air-sphere structures (as shown in Figure 2b). In the bar diagram it can be seen that both materials show a signal, an indication that titanium as well as zirconium are present in these areas. There is variation in the distribution: at positions 1 and 2 titania appears to be the main element present, as expected from the calculated chemical composition of 76%/24% (v/v) titania/zirconia. On the other hand, at positions 4 and 5 the zirconium signal is much stronger, suggesting that here zirconia is the majority. Position 3 was determined with SEM to be a closed area covered with bulk

(16) Holland, B. T.; Blanford, C. F.; Do, T.; Stein, A. *Chem. Mater.* **1999**, *11*, 795−805.
(17) Yan, H.; Blanford, C. F.; Holland, B. T.; Smyrl, W. H.; Stein, A. *Chem. Mater.* **2000**, *12*, 1134−1141.
(18) Dong, W. T.; Bongard, H. J.; Marlow, F. *Chem. Mater.* **2003**, *15*, 568−574.
(19) Reed, S. J. B. *Electron Microprobe Analysis*, 1st ed.; Cambridge University Press: New York, 1975; Chapter 13.
(20) The Monte Carlo simulation was kindly performed by Mr. Ton Gortenmulder of Leiden University.

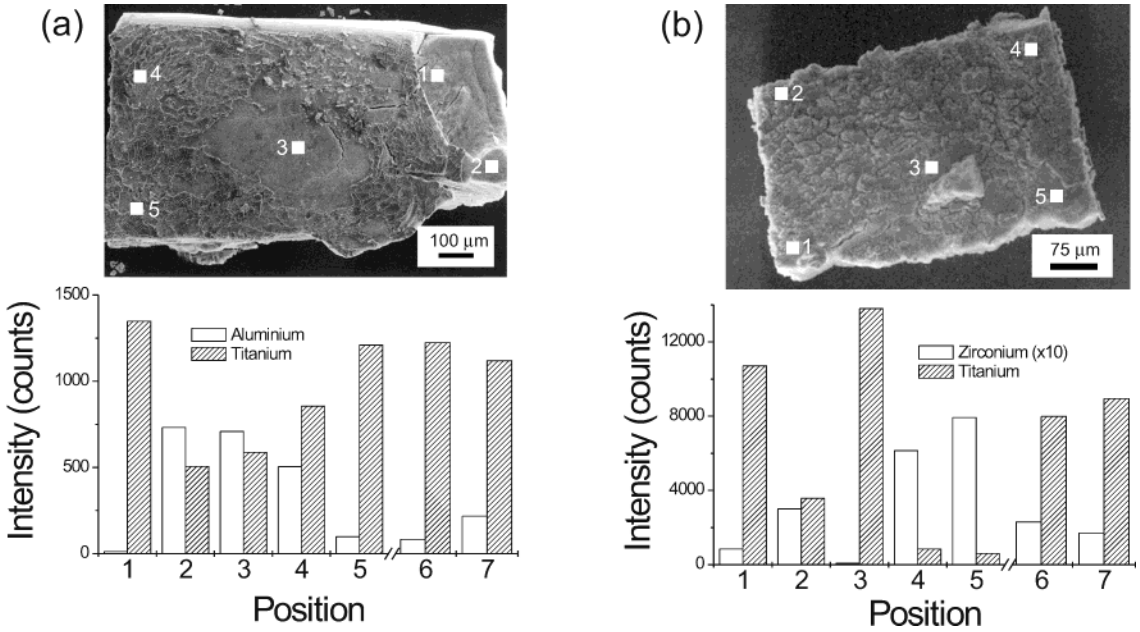

Figure 3. Bar diagrams (a and b) of the measured intensities for the specific X-ray radiations of different elements present in the sample. The measurements were done at several positions on the sample, corresponding to the numbers in the SEM picture (insets). Positions 6 and 7 are from different samples. The examined areas consist either of ordered or disordered air spheres or of bulk material that sometimes appears on the air spheres. (a) Data for alumina/titania samples, open bars for Al, hatched bars for Ti. (b) Data for zirconia/titania samples. Open bars are intensities for Zr multiplied by 10 because of the 10-fold lower detector efficiency. Hatched bars are for Ti.

material. Indeed, there is at this position hardly any signal from zirconium, indicating that this area consists mostly of titania. Considering that there is beneath this bulk titania layer a porous structure which can consist of both titania and zirconia, one might expect to see a zirconium signal. Since the excitation depth in bulk material is substantially lower than that in a porous structure, we are probably only exciting the bulk layer on top and do not reach the porous structure at all, resulting in no signal from zirconium. Positions 6 and 7 are measured on a different sample made in the same preparation batch. Both areas consist of open air-sphere structures. Titanium as well as zirconium are present, with the titanium signal stronger as expected.

Generally, in the EDS−SEM experiments we find both infiltrated elements present in the air-sphere structures. Usually, titanium appears to be present in excess, as expected since titania is the main component in our samples (∼75% v/v). In some areas we found aluminum or zirconium in excess. These results demonstrate the inhomogeneity of the in-filling procedure. The observation that possible bulk material on the surface of the samples is mainly titania can be explained by the fact that the last infiltrations are done with the titania precursor. In this way the titania precursor had more chance to settle on the outside.

(3) Energy-Dispersive Spectroscopy with TEM. Since the EDS measurements done with SEM only investigates the homogeneity on a length scale of ∼100 μm, we also performed EDS via TEM. With EDS−TEM it is possible to probe within single air spheres. In Figure 4a,b two typical TEM pictures of an alumina/titania and a zirconia/titania sample are displayed. The samples were prepared by crushing an air-sphere crystal from the same preparation batch as used in the EDS−SEM experiments. In both TEM pictures remains of spherical air spheres are visible. We have performed measurements at different positions in an area with a maximum cross section of 500 nm. The bar diagram shows the volume fractions of the present elements at different positions in this 500-nm area (not all positions are visible on the image). The absorption properties are in these samples less important since only X-ray emission from one or two layers is detected. Therefore, we used the measured intensities to calculate the volume percentages (with the program Quantex+ 1.6). A correction is done for different detection sensitivities of the different elements. All positions were interstitials such as position 3 in Figure 4a and positions 1 and 2 in Figure 4b, except position 4 in Figure 4a which represents an edge between two adjacent air spheres. From the displayed volume percentages in Figure 4a,b it is obvious that there is a large variation in the ratio of the elements. In Figure 4a aluminum and titanium at positions 1 and 2 show a rather evenly distributed volume fraction at variance with the bulk composition. These positions are less than 300 nm away from positions 3 and 4 where the ratios are significantly different. At these positions the titanium is the main component, which is expected on the basis of calculations on chemical compositions. In Figure 4b on positions 1 and 2 the ratios of zirconium and titanium hardly varies. Surprisingly, zirconium is found as the main component at these positions. At position 3, however, an interstitial that is only 200 nm away from position 2 (not shown in the TEM picture), titanium is the major element. These results demonstrate that, even within single air spheres, that is, on ∼100-nm lengths, the materials are not homogeneously distributed. To check whether this result was representative, we did measurements at more positions at different pieces of crushed material. In these experiments we observed similar inhomogeneity. Although the technique of successive infiltrations with different oxide precursors

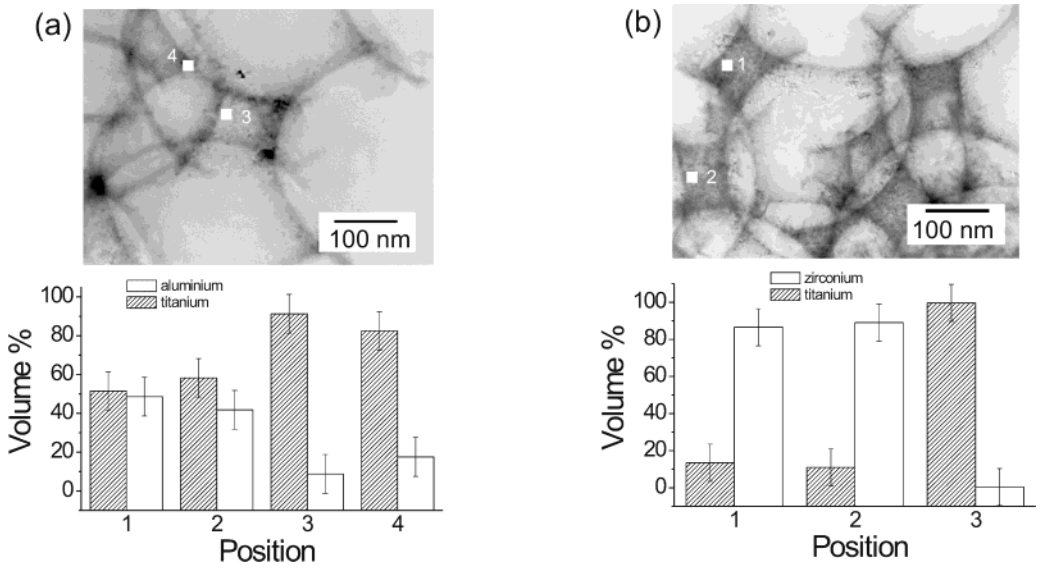

Figure 4. Bar diagrams (a and b) of the measured atom percentages for the specific X-ray radiations of Al and Ti in an alumina/titania air-sphere crystal (a) and Zr and Ti in a zirconia/titania air-sphere crystal (b). The measurements were done at several positions on the sample, corresponding to the numbers in the TEM picture (insets). Positions 1 and 2 in (a) and position 3 in (b) are outside the range of the photograph. Open bars represent Al or Zr and hatched bars Ti.

results in well-ordered mixed oxide air-sphere crystals, the distributions of the oxides is clearly not even throughout one sample.

We additionally observed that the titania present in the alumina/titania and the zirconia/titania sample was crystalline. This could be seen from crystallographic patterns that are caused by interference of the lattice planes. These patterns are visible in TEM pictures with a higher magnification and were also observed for zirconia, indicating crystallinity of both metal oxides. Additional X-ray experiments (results not shown here) confirm that alumina is amorphous, titania is in the anatase form, and zirconia is in the cubic form.

Discussion

This paper reports on the spatial distribution of constituent materials in air-sphere crystals. We have observed an extreme spatial inhomogeneity in air-sphere crystals prepared via successive infiltrations. With the naked eye inhomogeneities on the millimeter scale were observed, whereas with EDS−SEM inhomogeneities on the ∼100-μm scale were surveyed. Even on a single air-sphere level, that is, ∼100 nm, inhomogeneity in material distribution was measured with EDS-TEM. The ratio between the two present materials was varying from pure material A, via a mixed ratio A/B, to a pure material B in several positions in the crystal, apparent on all three length scales.

Differences in spatial distribution on the millimeter and 100-μm scale can indicate that the oxide precursor does not infiltrate homogeneously in the opal template. During each infiltration parts of the template may be infiltrated completely and other parts may not be infiltrated at all, as was also observed by the eye. Let us consider the in-filling process; the liquid is infiltrated via capillary forces into the opal. Since an opal experiences shrinkage during drying from the colloidal crystal, it displays cracks often in the vertical direction (see ref 9). Exactly these vertical cracks are in-filled first via capillary forces. As time proceeds in a matter of seconds, the bulk of the opal is infiltrated as well, also via capillary forces. Some parts however stay empty, and the precursor solution does not wet the polystyrene surfaces over here. Since our samples are infiltrated at least five times to obtain a reasonable filling fraction, it is not surprising that such inhomogeneous infiltration may result in compositional variations throughout one sample. Additionally, parts of the opal that are already infiltrated and have reacted can block these areas for following infiltrations.

Since the precursor and the diluting solvent are already mixed in advance, no diffusion of the precursor in the solvent is expected. During the infiltration process the mixture is diffusing with a constant flow between the spheres and the composition of the mixture is not expected to change.

With EDS−TEM inhomogeneities on an even shorter length scale were observed. Differences in the ratio between the two present materials were seen within single air spheres, corresponding to length scales of ∼100 nm. These inhomogeneities cannot likely be ascribed to inhomogeneous infiltration; therefore, we should consider other possibilities of inhomogeneity, namely, a redistribution of the materials during the evaporation, reaction, or calcination processes.

Evaporation Process. After each infiltration process the redundant solvent (ethanol or propanol) that is used for diluting the precursor is evaporated in a constant nitrogen flow. During this evaporation the precursor becomes more concentrated. Since the precursor solution wets the polystyrene surface and the formation of air spheres is surface templating, the remaining pure precursor is expected to stick to the polystyrene. We should however consider diffusion of the precursor during the evaporation of ethanol. The molecules nearby the sample surface will probably evaporate first and therefore the amount of precursor will increase relatively. In this way a concentration gradient can occur and diffusion of precursor to lower concentration areas, that is, the inner part of the crystal, can develop. We

think, however, that it is very unlikely that inhomogeneities will occur at this stage.

Reaction Process. The sample from which all the alcohol has evaporated is next exposed to water and the precursor hydrolyzes. During this hydrolysis the alkoxy groups are replaced by hydroxyl groups and the precursor condensates. The material solidifies on the surface of the polystyrene spheres. This reaction step is a nucleation step, the material changes from a fluid to a solid, and a redistribution can take place. During this density change inhomogeneities are likely to originate since the nucleation takes place at several different positions separately. Once the material is nucleated, it is a solid and diffusion will likely not take place anymore.

Calcination Process. During the calcination process the polystyrene is gasified and simultaneously the metal oxide is crystallized. First, the infiltrated opal is heated slowly to 80 °C; at this temperature the remaining alcohol, produced by the hydrolysis, is evaporated. Next, the sample is heated with 1 °C/min to a higher temperature, usually 450 °C. Above 100 °C the remaining water starts to evaporate and the hydrolyzed precursor of the metal oxide, that is, the solid pre-stage, starts to dehydrate. Above 300 °C the polystyrene starts to decompose, and above 350 °C all the polystyrene is removed; see Yan et al.[17] At these higher temperatures the metal oxide is also densified: hydroxyl groups are eliminated and metal−oxygen−metal bonds begin to form. The metal oxide crystallizes in crystallites with a maximum cross section of 50 nm.[9,13] This densification leads to a redistribution of the material and causes further inhomogeneities in material composition. For samples consisting of one oxide this can only lead to differences in volume fraction from point to point. These inhomogeneities however are much smaller than the optical wavelength, and thus hardly affect photonic crystal behavior.

Since our samples consist of two materials, redistribution of the material during the crystallization process is of major importance. If crystallization processes occur, it is not unlikely that the materials are redistributed from one position to another in order to form a denser composition. In the alumina/titania sample the alumina stays amorphous and the titania becomes crystalline. The alumina present between domains of titania may disturb the crystallization process and the materials are preferably redistributed. This also holds for the zirconia/titania sample. Both materials crystallize during the heating, likely at different temperatures, and therefore may also be separated; for titania the exothermic peak is observed at 404 °C,[21] while for zirconia a strong exothermic peak is observed at 430 °C for metastable cubic zirconia.[22]

An important consequence of the inhomogeneous distribution of the oxides can be the spatial variation of the average refractive index in photonic crystals since both alumina and zirconia have lower refractive indices than titania. Calculating the variation in average refractive index by comparing a composition of 100% titania and a composition of 100% alumina, we obtain a variation of the average refractive index, and thus of the Bragg diffraction wavelength, that is at the most 7% based on a porosity of 90%. Such an extreme variation is of the order or less than the width of the photonic stop bands. Therefore, an inhomogeneous distribution of oxides appears to be a minor issue for many photonic applications. When materials with a more distinct refractive index are applied, however, larger variations should be considered.

Conclusion

We have produced highly ordered composites consisting of macropores in a solid backbone made of mixed oxides. We have characterized the quality of the samples with scanning electron and optical microscopy, from which we conclude that the long-range order of these mixed oxide air-sphere crystals is of high quality.

Our investigation is a first step to obtain insight into the homogeneity of air-sphere crystals prepared via infiltration of artificial opals with liquid precursors. Awareness of inhomogeneities in such infiltration processes is very important when control in distribution of material is desirable.

Since the technique of successive infiltrations results in titania air-sphere crystals with an inhomogeneous shell of insulating material on the inner spheres, these composites are unsuited for dynamic spontaneous emission experiments on semiconductor (titania) photonic crystals. Because of the possible inhomogeneity of the layered mixed oxide air-sphere crystals, infiltrated light emitters such as dye molecules may experience different environments, varying from unshielded to shielded semiconductor surface. As a result, time-resolved measurements may reveal a distribution of lifetimes both from molecules that are quenched by electron transfer to the semiconductor surface and molecules that are shielded. Such a distribution will impede the interpretation of lifetimes related to photonic band gap effects.[23] For photonic crystals consisting of pure elemental materials, electron transfer can be prevented by other means. For instance, photonic crystals consisting of Si[24] or Ge[25] can be shielded by oxidizing the inner surface, resulting in insulating SiO_2 and GeO_2 layers, respectively.

All inhomogeneities discussed in our investigation were observed in air-sphere crystals prepared via a liquid precursor infiltration. For crystals with a compound backbone prepared via gas-phase infiltration, for example, chemical vapor deposition of GaAs or GaP,[26] the diffusion process would be different. Nevertheless, inhomogeneities may also occur and are an interesting subject for further investigation.

Acknowledgment. We thank Ton Gortenmulder and John Mydosh (Leiden University) for experimental

(21) Zhou, Q. F.; Wu, S. H.; Zhang, Q. Q.; Zhang J. X.; Chen, J.; Zhang, W. H., *Chin. Phys. Lett.* **1997**, *14*, 306−309.

(22) Colón, G.; Avilés, M. A.; Navío, J. A.; Sánchez-Soto P. J. *J. Therm. Anal. Cal.* **2002**, *67*, 229−238.

(23) Koenderink, A. F.; Bechger, L.; Schriemer, H. P.; Lagendijk, A.; Vos, W. L. *Phys. Rev. Lett.* **2002**, *88*, 143903.

(24) Blanco, A.; Chomski, E.; Grabtchak, S.; Ibisate, M.; John, S.; Leonard S. W.; Lopez, C.; Meseguer, F.; Míguez, H.; Mondia, J. P.; Ozin, G. A.; Toader, O.; van Driel, H. M. *Nature* **2000**, *405*, 437−440.

(25) Van Vught, L. K.; Van Driel, A. F.; Tjerkstra, R. W.; Bechger, L.; Vos, W. L.; Vanmaekelbergh, D.; Kelly, J. J. *Chem. Commun.* **2002**, 2054−2055.

(26) Farthing, J. S.; Buhro, W. E.; Bechger, L.; Vos, W.; Wijnhoven, J. E. G. J. *Abstr. Am. Chem. Soc.* **2001**, *221*, 388.

help with SEM−EDS, Wijnand Takkenberg (University of Amsterdam) for experimental help with SEM, and Léon Woldering for assistance with TEM−EDS and reading the manuscript. We thank Femius Koenderink for useful discussions and Ad Lagendijk for encouragement and support. This work is part of the research program of the Stichting voor Fundamenteel Onderzoek der Materie (FOM), which is financially supported by the Nederlandse Organisatie voor Wetenschappelijk Onderzoek (NWO). This work was initiated at the Van der Waals-Zeeman Institute at the University of Amsterdam.

CM035373O